



Systemic cellular viroimmunotherapy for canine high-grade gliomas

Ana Cloquell ¹, Isidro Mateo ^{1,2}, Stefano Gambera ^{3,4}, Martí Pumarola,⁵
Ramon Alemany,⁶ Javier García-Castro ³, Ana Judith Perisé-Barrios ⁷

To cite: Cloquell A, Mateo I, Gambera S, *et al.* Systemic cellular viroimmunotherapy for canine high-grade gliomas. *Journal for ImmunoTherapy of Cancer* 2022;**10**:e005669. doi:10.1136/jitc-2022-005669

► Additional supplemental material is published online only. To view, please visit the journal online (<http://dx.doi.org/10.1136/jitc-2022-005669>).

AC and IM contributed equally. JG-C and AJP-B contributed equally.

Accepted 19 October 2022

ABSTRACT

Background Oncolytic viruses constitute a growing field of interest, both in human and veterinary oncology, given that they are particularly helpful for treating non-surgical tumors and disseminated cancer, such as high-grade gliomas. Companion dogs present malignant gliomas with biological, genetic, phenotypic, immunological, and clinical similarities to human gliomas. These features favor comparative approaches, leading to the treatment of canine oncological patients to achieve translational applications to the human clinic. The systemic administration of oncolytic viruses presents a challenge due to their limitations in effectively targeting tumors and metastases. Therefore, the aim of this study is to evaluate the safety and antitumor activity of a virotherapy used in spontaneous canine tumors.

Methods Ten dogs with high-grade rostrotentorial gliomas underwent weekly systemic endovenous cellular virotherapy with dCelyvir (canine mesenchymal stem cells infected with the canine oncolytic adenovirus ICOCAV17) for 8 weeks. Efficacy was determined in seven dogs according to the Response Assessment in Veterinary Neuro-Oncology criteria considering clinical status and MRI measurements. Medical history, physical and neurological examinations, and vaccination status were evaluated prior to and during follow-up. Safety was evaluated by physical examinations and hematological and biochemical changes in peripheral blood. Immune populations were analyzed by flow cytometry in peripheral blood and by gene expression and immunohistochemistry in the tumor microenvironment.

Results The treatment was well tolerated and major adverse effects were not observed. Two dogs had partial responses (76% and 86% reduction in tumor size), and 3/7 showed stable disease. ICOCAV17 was detected in peripheral blood in nine dogs, and a correlation between the ICOCAV17 particles and anti-canine adenovirus (CAV) antibodies was observed. ICOCAV17 was detected in 3/9 tumor tissues after necropsies. Regarding tumor-infiltrating lymphocytes, the dogs with disease stabilization and partial response tended to have reduced memory B-cell infiltration and increased monocyte/macrophage lineage cells.

Conclusions These findings indicate that dCelyvir is safe and presents efficacy in canine rostrotentorial high-grade gliomas. These data are relevant to the ongoing phase Ib regulated human clinical trial that is administering this virotherapy to children, adolescents, and young adults with diffuse pontine glioma. Celyvir should be further explored as a treatment in veterinary and human neuro-oncology.

WHAT IS ALREADY KNOWN ON THIS TOPIC

⇒ High-grade gliomas have a poor short-term prognosis, despite the use of the most advanced or aggressive therapies when possible, and the efficacy of oncolytic viruses is limited by difficulties in targeting brain tumors. Therapies, therefore, need to be improved to reach the brain.

WHAT THIS STUDY ADDS

⇒ The systemic endovenous treatment is safe, ensures that the virus is delivered to the brain tumor, and response evaluation suggest clinical efficacy.

HOW THIS STUDY MIGHT AFFECT RESEARCH, PRACTICE OR POLICY

⇒ These data are relevant to the ongoing phase Ib regulated human clinical trial that is already administering this virotherapy to children, adolescents, and young adults with diffuse pontine glioma.

BACKGROUND

Oncolytic viruses (OVs) as therapeutic agents constitute a growing field of interest, both in human and veterinary oncology with several ongoing clinical trials and promising results.¹ OVs can reverse the microenvironment's immunosuppressive status² and induce intratumoral immunostimulatory signals increasing immune cell infiltration.³ The virus' lytic activity induces the release of tumor neoantigens, leading to an antitumor response.^{4,5} Due to its nature and mechanism of action, adenovirus is effective in promoting immune response, controlling tumor growth, and improving survival.^{6,7} Conditionally replicating adenoviruses (CRADs) are an option for patients with cancer because CRADs have a selective potential for replication, achieving a successful viral cycle in tumor cells, resulting in cell destruction. Most CRADs rely on tumor-specific promoters to control the master key gene E1a and in deletions in domains of E1 genes that are needed to block cell cycle regulators such as pRB or p53. Due to the lack of function of such regulatory proteins in tumors, such deletion only has a detrimental effect on virus replication



© Author(s) (or their employer(s)) 2022. Re-use permitted under CC BY-NC. No commercial re-use. See rights and permissions. Published by BMJ.

For numbered affiliations see end of article.

Correspondence to

Dr Javier García-Castro; jgcastro@isciii.es

in normal cells but not in tumor cells. CRADs can also be genetically modified to enhance their infectivity and/or intratumoral spread.⁸

The use of CRADs can be particularly helpful for treating non-surgical tumors, such as high-grade gliomas.^{9,10} Glioblastoma multiforme (GBM) is the most frequent malignant primary brain tumor in dogs and humans, and the standard patient care includes incomplete surgical resection combined with radiation and/or chemotherapy; unfortunately, these treatments achieve a poor short-term prognosis in humans and dogs.¹¹ Treatment with CRADs has shown promising results in veterinary trials, and further in human clinical trials including a phase I using intratumoral injections of DNX-2401, showing clinical benefit in 12% of cases, with long-term survival in patients with recurrent high-grade gliomas, and a link to an immune-mediated response.^{12,13} Further, the infusion of OV DNX-2401 followed by radiotherapy in pediatric patients with diffuse intrinsic pontine glioma resulted in a reduction or stabilization of tumor size.¹⁴

Although CRADs have also been systemically administered, they have shown limited efficacy due to various barriers that viral particles encounter in targeting neoplastic lesions, such as neutralization in blood and liver uptake.¹⁵ Intracranial solid tumors are not always surgically accessible, and the intratumoral delivery of CRADs is not a feasible option for these patients in the regular clinic. To improve the systemic administration of CRADs, the use of mesenchymal stem cells (MSCs) as cellular carriers for CRADs in humans and dogs has been previously demonstrated.^{6,16} MSCs were infected *in vitro* with CRADs and employed as a ‘Trojan horse’, avoiding systemic immunity against the virus and even further reaching the tumor due to their tumor-homing capacity. This treatment, named Celyvir, has been demonstrated to be effective in humans and canine patients without secondary effects or toxicity.^{6,17}

The most complete study developed in the veterinary field have been performed using a canine oncolytic adenovirus named ICOCAV17.⁶ This CRAd has the same characteristics as the human oncolytic adenovirus ICOVIR17 (used in clinical trials as VCN-01): In particular, ICOCAV17 has four palindromic E2F to repress E1a promoter in normal cells though the E2F-pRB complex and to activate E1a expression in tumor cells through free E2F. In addition, the pRB binding domain of E1a has been deleted in ICOCAV17. To increase its antitumor potency this virus express hyaluronidase linked to the major late promoter and has an RGD motif inserted in the HI-loop of the fiber.¹⁸ In this regard, we previously published a veterinary clinical trial, in which 27 dogs with extracranial solid tumors were treated with canine Celyvir (dCelyvir) by using allogenic canine MSCs (dMSCs) infected with ICOCAV17, showing a response rate of 74%, including 14.8% of complete remission, with an excellent toxicity profile.⁶ The safety and efficacy of this treatment in canine intraparenchymal primary brain tumors have never been explored and remain unknown. The results could be

significantly different from those obtained in previous studies in dogs with extracranial tumors, given that the brain environment and the blood-brain barrier can play a role that could affect the clinical outcome. Therefore, it would be useful to describe the dCelyvir therapy effects in a brain tumor population.

Domestic dogs develop spontaneous neoplasms in the central nervous system (CNS),^{7,19–21} present intratumor heterogeneity, and have clinical and pathophysiological features and genetic changes equivalent to human CNS tumors.^{22,23} The conserved glioma drivers and aneuploidy have been identified as a hallmark of high-grade disease, showing high similarity especially between human pediatric and canine gliomas.¹⁹ In addition, dogs have an intact immune system and present similarities with humans in tumor immune infiltration, making them a valuable immunocompetent model.^{19,23–25}

Moreover, the absence of effective gold standards for managing high-grade gliomas in dogs^{11,26,27} makes these tumors excellent candidates for developing novel therapeutics, with the aim of obtaining responses allowing comparative approaches that favor a clinical translation of the findings from dogs to humans.^{19,20,28} Gliomas are one of the most common tumors in dogs, that represent 36%–70% of primary brain tumors in those animals, which have a poor prognosis due to the lack of an accessible and effective treatment for this disease. Radiotherapy is an expensive treatment and not recommended for some diffuse tumors (unless novel irradiation equipment is available, which unfortunately is not common), and benefit from resection surgery appears to be limited. Fortunately, the availability of advanced imaging for the diagnosis and follow-up, makes dogs excellent animal models to test novel therapeutic strategies, as immunotherapies.^{21,26} Therefore, veterinary trials with companion dogs are useful in translational research, and should take a position between basic research and human clinical trials.^{25,29,30}

The aim of this study was to evaluate the safety and efficacy of systemic infusions of dCelyvir and its immune-related response in canine patients with high-grade gliomas. The findings will allow us to address improvements in current therapies in human gliomas, leading us to propose the use of the therapy described here as a treatment for people with brain tumors, even as a first line of treatment. The findings reported here are indeed novel and the first to describe the therapy effects in patients with brain tumors.

MATERIAL AND METHODS

Patient selection

The study followed the ARRIVE guidelines 2.0, and the information can be found in the manuscript. The study’s inclusion criteria were as follows: (1) client-owned dogs with a single intra-axial rostromentorial mass suspected to be a high-grade glioma based on MRI findings; (2) no previous treatments except for palliative care with

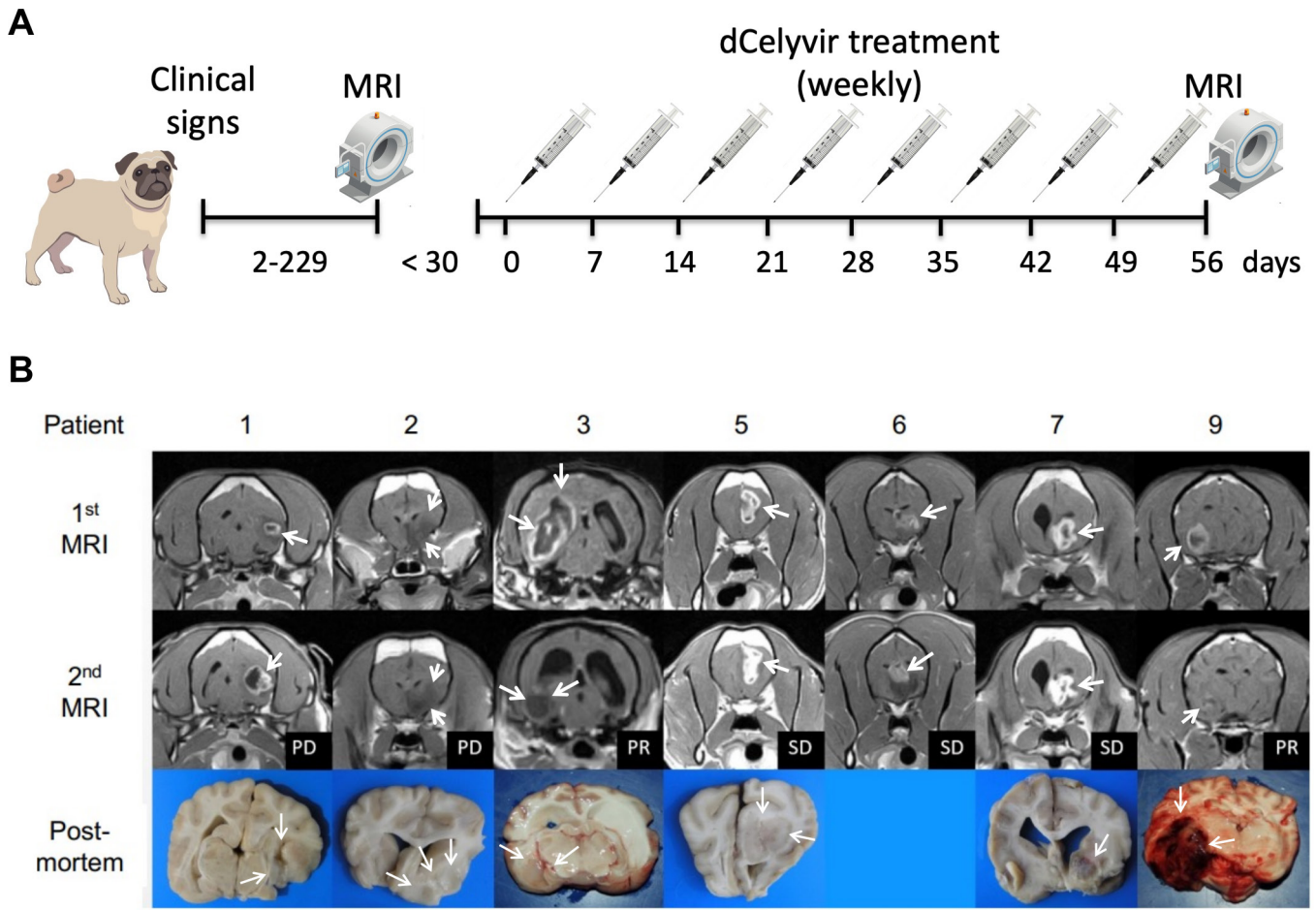


Figure 1 (A) Schematic representation of the dCelyvir treatment. (B) MRI and macroscopic tumor images from the dCelyvir-treated patients. MRI prior to dCelyvir treatment (first MRI), and 2 months after starting weekly treatment (second MRI) showing tumors (white arrows). Clinical benefit is indicated according to RAVNO criteria. Bottom figures show macroscopic tumor tissue (white arrows) in necropsies. PD, progressive disease; PR, partial response; RAVNO, response assessment in veterinary neuro-oncology; SD, stable disease.

anticonvulsants and/or prednisone; (3) good physical condition with no hematological or biochemical evidence of organ dysfunction; (4) a mild increase in liver enzymes with a normal bile acid stimulation test was considered acceptable in cases under corticosteroid or anticonvulsant therapy; and (5) dogs whose owners declined other therapeutic options such as surgery, radiotherapy, and chemotherapy. Dogs weighing less than 4 kg and dogs with concurrent neoplastic or inflammatory diseases were excluded.

Clinical study design

The trial followed a schedule of the weekly intravenous administration of dCelyvir at 0.5×10^6 dMSC/kg for 8 weeks, following the previously described protocol.⁶ To avoid anaphylactic reactions, dogs were pretreated with metamizol (30 mg/kg/IV) and difenhydramine (0.5 mg/kg/IV). Tumor reevaluation by MRI at 2 months (figure 1A). At diagnosis, all dogs received a tapering course of prednisone for 4 weeks, and phenobarbital was initiated and continued throughout the treatment in the dogs with seizures. The clinical outcome was defined according to the response assessment in veterinary

neuro-oncology (RAVNO) criteria with a modification³¹: lesions were measured even if their longest diameter was smaller than 10 mm. Treatment was discontinued in those dogs with progressive disease (PD) or severe biochemical abnormalities (such as elevation of serum liver enzyme's activity more than three times the upper normal limit). Those dogs with partial response (PR) or stable disease (SD) were selected for a second round of dCelyvir (four doses, every 2 weeks). Adverse effects were defined by the veterinary cooperative oncology group for common terminology criteria of adverse events in dogs and cats. The dogs were followed-up until death, at which point they underwent a necropsy within 24 hours. Samples from the tumor, the unaffected contralateral hemisphere, and the liver were used to perform histopathology and immunohistochemistry, or snap frozen to analyze the RNA expression.

Cell culture and dCelyvir preparation

Isolation and characterization of dMSC from the adipose tissue of healthy donor dogs, were performed as previously described.⁶ The presence of mycoplasma (MycoAlert

Mycoplasma Detection Kit, Lonza) and the preparation of dCelyvir treatment were as previously described.⁶

MRI and RAVNO criteria

Imaging studies were performed at pre-treatment and 2 months after the first dCelyvir treatment using an MRI unit (Hitachi Airis Mate 0.2T model; Tokyo, Japan). The tumor size was calculated considering the contrast-enhancing lesion (online supplemental figure S1A); when no enhancement was detected, the size was calculated by comparing the parenchymal intensity patterns with the normal anatomy (online supplemental figure 1B-C). Peritumoral edema (online supplemental figure 1D-E) and the midline shift were measured (online supplemental figure 1F). Clinical outcomes were defined by RAVNO criteria as follows: complete response, stable or improved clinical status not receiving steroids, elimination of all enhancing tumors and stable or decreased T2W/fluid-attenuated inversion recovery (FLAIR) lesion burden; PR: $\geq 50\%$ decrease in the contrast enhancing lesion burden in patients with stable or improved clinical status; SD $< 50\%$ decrease or $< 25\%$ increase in enhancing tumor size in a patient with stable or improved clinical status requiring stable or decreased steroid doses; and PD $\geq 25\%$ increase in enhancing tumor in T2W/FLAIR images, new lesions and/or clinical deterioration. For further details regarding the MRI, see online supplemental information.

Histopathology, diagnosis, and immunohistochemistry

The morphological evaluation was performed on formalin-fixed, paraffin-embedded sections stained with hematoxylin and eosin in eight necropsies. Tumors were classified according to the 2007 criteria of the WHO for human CNS tumors³² and the subsequently revised diagnostic scheme for canine gliomas.^{19,28,33} Samples were evaluated for the presence of necrosis, extracellular matrix degradation, vascular proliferation, mucinous secretion, and hemorrhages.

Immunohistochemistry was performed using primary antibodies to detect glial fibrillar acidic protein (Dako Z0334; Glostrup, Denmark), oligodendrocyte transcription factor 2 (Olig2, Merck Millipore AB9610; Billerica, Massachusetts, USA), CD3 (Dako A0452; Glostrup, Denmark), CD20 (Thermo Fisher PA5-32313; Waltham, Massachusetts, USA), FOXP3 (forkhead box P3, eBioscience 14-7979; Waltham, Massachusetts, USA) and ICOCV17 (anti-Ad5 Abcam ab6982). Stained tumor slides were assessed using image analysis software (NanoZoomer Digital Pathology; Hamamatsu, Japan). A number of CD3⁺, CD20⁺ and FOXP3⁺ lymphocytes were determined. For further details, see online supplemental information.

Cytokine analysis

Blood samples were obtained at days 0, 1, 2, and 3 and prior to every weekly dCelyvir infusion. Samples were collected in BD vacutainer separator tubes (BD

SSTII-Advance), and serum was obtained and frozen at -20°C . Quantification of interleukin (IL)-2, IL-6, IL-7, IL-8, IL-10, IL-15, IL-18, interferon (IFN)- γ , CXC chemokine ligand (CXCL)10, granulocyte-macrophage colony-stimulating factor (GM-CSF), CC chemokine ligand (CCL)2 and keratinocyte-derived chemokine (KC)-like were performed with an Immunology Multiplex Assay (Milliplex MAP Canine Cytokine/Chemokine Magnetic Bead Panel, Millipore; Darmstadt, Germany) following the manufacturer's protocol and were analyzed using Luminex technology.

Antiviral-specific antibodies

Blood samples were collected in BD vacutainer plasma separator tubes (BD PSTII); then plasma was obtained and frozen at -20°C until analysis. To determine specific antibodies (IgG) against canine adenovirus (CAV), a solid-phase ELISA was performed (ImmunoComb Canine VacciCheck, Biogal Galed Laboratories Acs.; Kibbutz Galed, Israel) following a previously described protocol.⁶

DNA extraction from blood and tissues and qPCR analysis

Blood samples were collected in PAXgene Blood DNA tubes and processed using the QIAamp DNA Blood Mini Kit (Qiagen; Madrid, Spain) following the manufacturer's instructions. Tumors from necropsies were snap frozen at -80°C as dried pieces. Tissue samples were introduced into a metal cylinder submerged in liquid nitrogen and ground thoroughly with a pestle until they were completely pulverized. DNA was isolated using the QIAamp DNA Mini Qit (Qiagen). DNA quantification and purity (A260/280 and A260/230) were analyzed with a Nanodrop 2000 spectrophotometer (Thermo Scientific). Dilutions of ICOCV17 from 10^8 to 10^3 vp/mL in blood from healthy donors were used for the standard curve. Samples were analyzed in triplicate by the quantitative real-time PCR (qRT-PCR) 7500 Fast (Applied Biosystems; Madrid, Spain) using the Premix Ex Taq (Clontech; Saint-Germain-en-Laye, France), with forward primer ($0.5\ \mu\text{mol/L}$) 5'TGTGGGCCTGTGTGATTCCT-3'; reverse primer ($0.5\ \mu\text{mol/L}$) 5'-CCAGAATCAGCCTGAGTGCTC-3'; and 10 pmol of Taqman probe FAM-CTCGAATCAGTGTCAGGCTCCGCA-TAMRA, which identified the E1A region. The qRT-PCR conditions were as follows: holding stage 10 min at 95°C , cycling stage 15 s at 95°C and 1 min at 60°C , repeated 40 times. Analysis was performed using the 7500 Software V.2.0.6 (Applied Biosystems).

Flow cytometry

Blood samples were collected in a BD vacutainer K3EDTA. Samples were incubated with human FcR Blocking (Miltenyi; Cologne, Germany) for 10 min at room temperature and incubated for 20 min at 4°C with directly conjugated antibodies diluted in phosphate-buffered saline with 1% fetal bovine serum. Samples were incubated with QuickLysis buffer (Cytognos; Salamanca, Spain) to lyse erythrocytes. The acquisition and

analysis were conducted in a MacsQuant10 Flow Cytometer (Miltenyi). The antibodies employed and the flow cytometry gating strategy of the immune subpopulation analysis in dog-derived samples have been previously described.⁶

RNA extraction, gene expression, and tumor-infiltrating immune cell profile

Tumor tissues were snap frozen at -80°C , and RNA was isolated using the RNeasy Mini Kit (Qiagen) and was analyzed with a Nanodrop 2000 spectrophotometer (Thermo Scientific). The RNA Integrity Number was evaluated using the Bioanalyzer RNA 6000 Nano assay, and samples with RIN values higher than 8.6 were used. Tumor RNA expression was analyzed by GeneChip Canine Gene V.1.0 ST Array (Affymetrix). Data were analyzed using Transcriptome Analysis Console Software. Tumor-infiltrating leukocyte cell fractions of 6 tumors were estimated from bulk RNA expression data employing a CIBERSORT algorithm (<https://cibersort.stanford.edu>).³⁴ The microarray expression matrix of canine tumors was preprocessed to match human gene identifiers with canine orthologues. Leucocyte infiltration was estimated using a validated leukocyte gene signature matrix (LM22); canine orthologues matched 85% of the LM22 gene signature matrix. Analysis was performed in relative mode, with 100 permutation runs and without quantile normalization. The resulting cellular fractions were collapsed from 22 to 11 cell types based on their lineage, as previously described.³⁴

Statistical analysis

The data were graphed and analyzed with Excel 2013 (Microsoft Office 2013) and Prism (GraphPad) Software. Comparisons between quantitative variables were performed with Wilcoxon's rank-sum test, and the Mann-Whitney statistic for samples with non-normal distribution. Differences were considered significant at $*p<0.05$;

$**p<0.01$ and $***p<0.001$. To test statistical association between two continuous variables, a Pearson's correlation coefficient test was performed. A two-way analysis of variance and Bonferroni's multiple comparison tests were used to analyze CIBERSORT results.

RESULTS

Canine patient demographics and clinical status

Ten dogs were enrolled for the dCelyvir therapy. Brachycephalic breeds were overrepresented (six French bulldogs, two Boxers, and one English bulldog). There were seven males and three females with a median age of 8 years (6–10 years) and a mean weight of 17 kg (4.4–38.8 kg). All the dogs had been vaccinated against CAV2 (table 1), all had experienced seizures, and seven of them showed other prosencephalic signs (abnormal mental status, contralateral hemiparesis, menace response deficits and/or abnormal facial sensation). The mean period from first neurological signs to diagnosis was 40 days (online supplemental table S1). Prednisone treatment was maintained during the entire treatment in five dogs and the other five were treated intermittently (overall, the dogs received prednisone during 73% of the treatment time). All the dogs, except one, received phenobarbital during the entire dCelyvir treatment.

Safety and toxicity of dCelyvir

In most of the dogs, the dCelyvir treatment was well tolerated, except for one dog who showed a forelimb swelling contralateral to the site of venous catheterization after the first dCelyvir administration. The adverse event was resolved 48 hours after treatment with a single dose of meloxicam (0.2 mg/kg subcutaneous) and difenhydramine (0.5 mg/kg intramuscular). Two dogs showed mild fatigue after treatment on two occasions each.

Table 1 Patient characteristics, treatment, clinical outcome, and tumor characterization

Patient	Age	Breed	Gender	CAV vacc.	dCelyvir doses	RAVNO	Tumor location	Diagnosis
1	8	French Bulldog	M	8	8	PD	Temp.	Olig. III
2	6	French Bulldog	M	3	11	PD	Frontal	Olig. III
3	7	Poodle	M	1	8	PR	Temp.+Occ.	Olig. III
4	9	English Bulldog	F	11	1	N/A	Temp.+Th.	N/A
5	9	Boxer	F	35	12	SD	Frontal	Olig. III
6	9	Boxer	M	5	14	SD	Frontal	GBM
7	10	French Bulldog	M	4	12	SD	Frontal+Th.	GBM
8	6	French Bulldog	M	5	5	N/A	Frontal+parietal + Temp.+Th.	Olig. III
9	8	French Bulldog	F	10	17	PR	Parietal+Th.	N/A
10	6	French Bulldog	M	3	4	N/A	Frontal	Olig. III

Age in years; CAV vaccination in months.

CAV, canine adenovirus; F, female; GBM, glioblastoma multiforme; M, male; N/A, not available; Occ., Occipital; Olig. III, oligodendroglioma grade III; PD, progressive disease; PR, partial response; RAVNO, response assessment in veterinary neuro-oncology; SD, stable disease; Temp., temporal; Th., thalamus.

There were no significant changes in the complete blood count during the treatment (online supplemental figure S2A). Total protein, albumin, globulin, glucose, urea, creatinine, Na⁺, K⁺ and Ca⁺⁺ levels also remained within the reference ranges during the follow-up (online supplemental figure S2B). However, patient 3 had neutrophilic and monocytic leucocytosis (online supplemental figure S2A) and increased urea levels (online supplemental figure S2B) before treatment, which were progressively normalized after the second week of treatment.

Liver enzymes were analyzed to assess whether the dCelyvir treatment affected liver function. Alkaline phosphatase (ALP) levels were increased before the treatment in five dogs and remained elevated in three of them until death (online supplemental figure S2C). Patient 5 was the only one who also showed increased ALP and aspartate transaminase levels during treatment (online supplemental figure S2C). Serum alanine transaminase levels were over the baseline in eight dogs before treatment but were reduced or maintained during treatments, except for patient five who showed a slight increment (online supplemental figure S2C). Most dogs developed neurological complications during treatment (abnormal mental status, seizures, and changes in behavior), which are normally associated with the presence of the brain tumor and could therefore not be attributed to the treatment itself.

The patient 4 experienced severe elevation of liver enzymes attributed to medical treatment with steroids and phenobarbital prior to the dCelyvir treatment. The blood analysis performed 7 days after the treatment showed bilirubinemia, hypoalbuminemia, mild anemia, leukocytosis, and increased bile acids. Due to deteriorating clinical signs and liver dysfunction, the dCelyvir treatment was discontinued, and the dog was euthanized due to experiencing renal and hepatic failure. The final histopathological classification was not available because necropsy was not allowed.

Imaging findings

Before the dCelyvir treatment, all MRI studies showed the classic radiological features of high-grade gliomas, including the presence of a single intra-axial mass mainly hypointense in T1-weighted images and hyperintense in T2-weighted and FLAIR (online supplemental figure S1). The tumor location varied, affecting multiple lobes (or one lobe and the thalamus) in five dogs (table 1). Contrast enhancement was severe in a ring-like pattern in nine dogs; however, the patient 2 did not have any enhancement (figure 1B). Before treatment, mass areas ranged from 57 mm² to 670 mm² (mean 281 mm²), and most cases showed mass effect evidenced as ventricular collapse (8/10) and/or midline shift (9/10), ranging from 0 mm to 5.7 mm (mean 3mm) (online supplemental table S1). Perilesional edema was also observed in most dogs (9/10).

Patient 3 was also imaged by CT after euthanasia to investigate the cause of the jaw pain observed several

weeks before, which could not be attributed to the glioma. The images showed a lesion in the right temporal lobe (online supplemental figure S3A, asterisk) and bilateral bone resorption (online supplemental figure 3B,C, arrows) affecting the orbital area of the frontal bones (online supplemental figure S3D, arrows). Also, the wings of the presphenoid and basisphenoid bones and the ventral area of the temporal bone were affected (online supplemental figure S3E). The bone resorption was more severe ipsilateral to the intracranial tumor. Three dogs subsequently added to the study underwent CT study postmortem even if they did not have any clinical signs suggesting osteolysis of the cranial bones. Two of them (patients 5 and 7) showed bone resorption. Patient 5 showed involvement of the internal lamina of the frontal bone adjacent to the tumor (online supplemental figure S3F). Patient 7 showed bone resorption of the orbital area of the left frontal bone and ethmoid bone (online supplemental figures 3G,H) and bilaterally in the temporal bones, despite the tumor being in the left frontal lobe.

Clinical outcome

Seven dogs survived more than 2 months after starting the treatment, having a second MRI evaluation (figure 1B). Tumor size and midline shift reduction were observed in 57% (4/7) and 43% (3/7) of dogs, respectively (online supplemental table S1 and figure 2A). The clinical benefit of these seven dogs was evaluated following the RAVNO criteria: two dogs presented PD, three SD, and two PR, showing a reduction of 76% and 86% in tumor size (online supplemental table S1, figures 1 and 2A). The main radiological features of the lesions (type of enhancement, peritumoral edema, and mass effect) changed during the follow-up in two dogs, one of which presented a moderate peritumoral edema prior to treatment that was undetectable after 2 months. The other peritumoral edema progressed from moderate to severe. Four dogs died naturally and six were euthanized due to clinical deterioration at the owner's request. The median survival time (MST) was 128 days from clinical onset, 123 days from diagnosis, and 90 days from the start of the dCelyvir treatment (online supplemental table S1 and figure 2B,C). The number of dCelyvir doses ranged from 1 to 17 (median of 8) (table 1). There was no correlation between survival time (from the start of treatment) and tumor size evaluated at pretreatment (figure 2D) or after 2 months of weekly treatment (figure 2E); and the survival time lacked any correlation with the tumor growth (figure 2F). However, there was a positive correlation ($r=0.8455$) between the number of dCelyvir doses and survival time (figure 2G).

The final diagnosis was performed by immunohistochemical study in eight dogs after necropsy (two dogs were not available for necropsy). All tumors were diagnosed as high-grade gliomas: 6 of them were grade III oligodendrogliomas and two were GBM (grade IV astrocytomas) (table 1 and online supplemental figure S4).

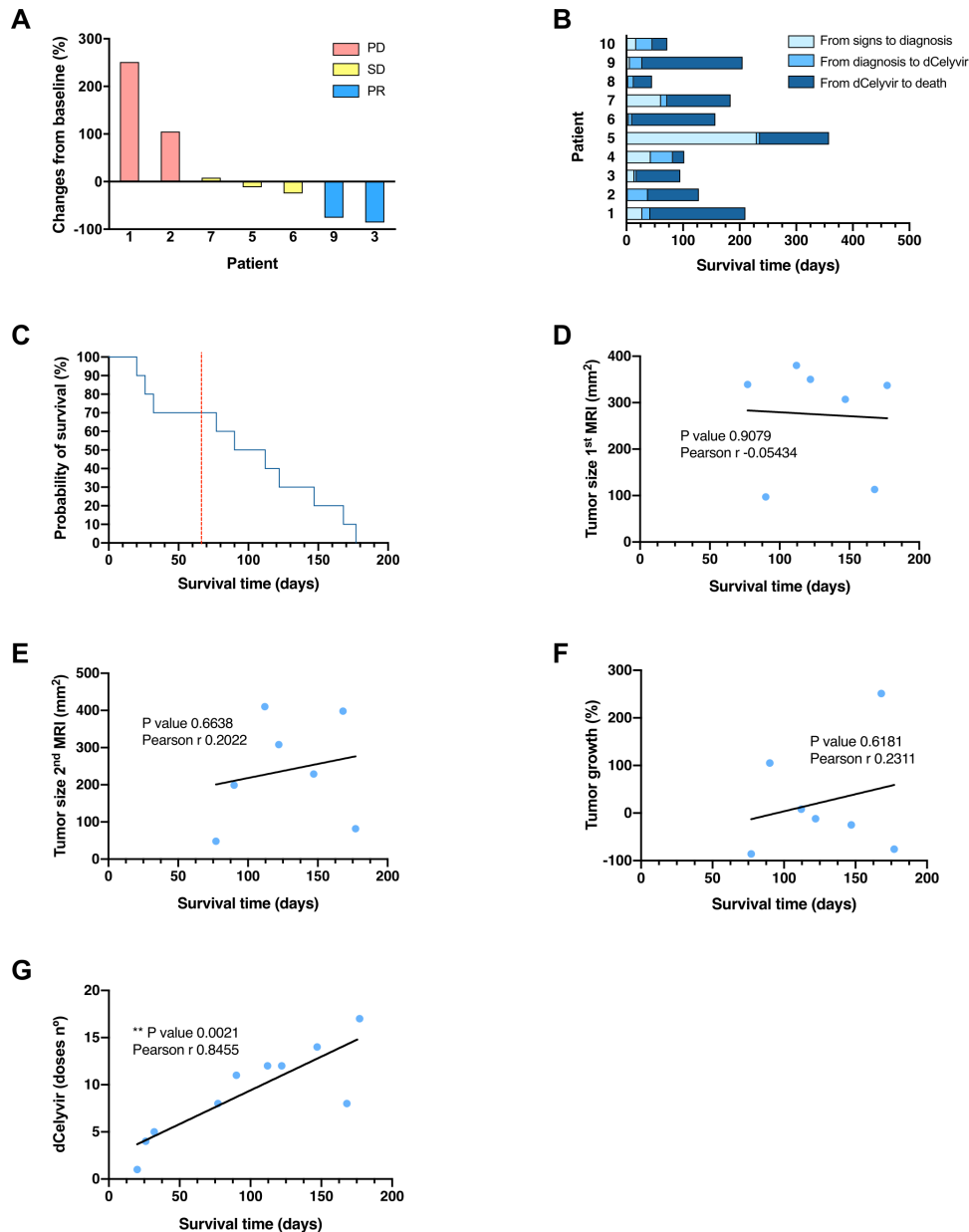


Figure 2 Tumor growth and survival time from the dCelyvir-treated patients. (A) Waterfall plot showing changes in tumor size. Tumor growth from baseline (first MRI) to 2 months after starting the dCelyvir treatment (second MRI) is shown for each patient. (B) Survival time. Bar plot showing the total survival time for each patient. The days from symptom onset to diagnosis, from diagnosis to starting dCelyvir treatment, and from treatment to death are indicated for each patient. (C) Survival analysis. Kaplan-Meier curve showing the probability of survival for dCelyvir-treated dogs (blue line) starting with day of treatment up to death. The dashed red line indicates the MST according to the literature and the historical cases treated with resective surgery. (D–G) Correlation analysis between survival time and tumor size at first MRI (D), at second MRI (E), tumor growth (F), and dCelyvir dose (G) calculated by Pearson's correlation coefficient (r). Individual values (blue dots) and regression lines are shown. ** $p < 0.005$. MST, median survival time; PD, progressive disease; PR, partial response; SD, stable disease.

Virus and antiviral antibody detection

The oncolytic adenovirus ICOCAV17 was detected in the blood of all of the treated dogs that were analyzed ($n=9$) (figure 3A). Five of them showed the highest viral particles 2 days after the first treatment, showing a steady reduction until 14 days after the first treatment. Two dogs achieved the highest values on the third day after the first doses; the presence of the virus in the blood samples subsequently decreased. Lastly, patient 5 (the one with the longest time

since the last vaccination) showed the highest virus titer 7 days after the second dose (d14) (figure 3A and table 1); however, this dog presented a similar anti-CAV2 antibody titer to that of the other dogs that had been vaccinated more recently (figure 3B). Further, ICOCAV17-positive cells were detected inside gliomas from necropsies in 3 dogs (1, 6, and 10) (figure 3D). All the treated dogs showed anti-CAV2 antibodies before the dCelyvir treatment, which increased gradually from the first dose; after

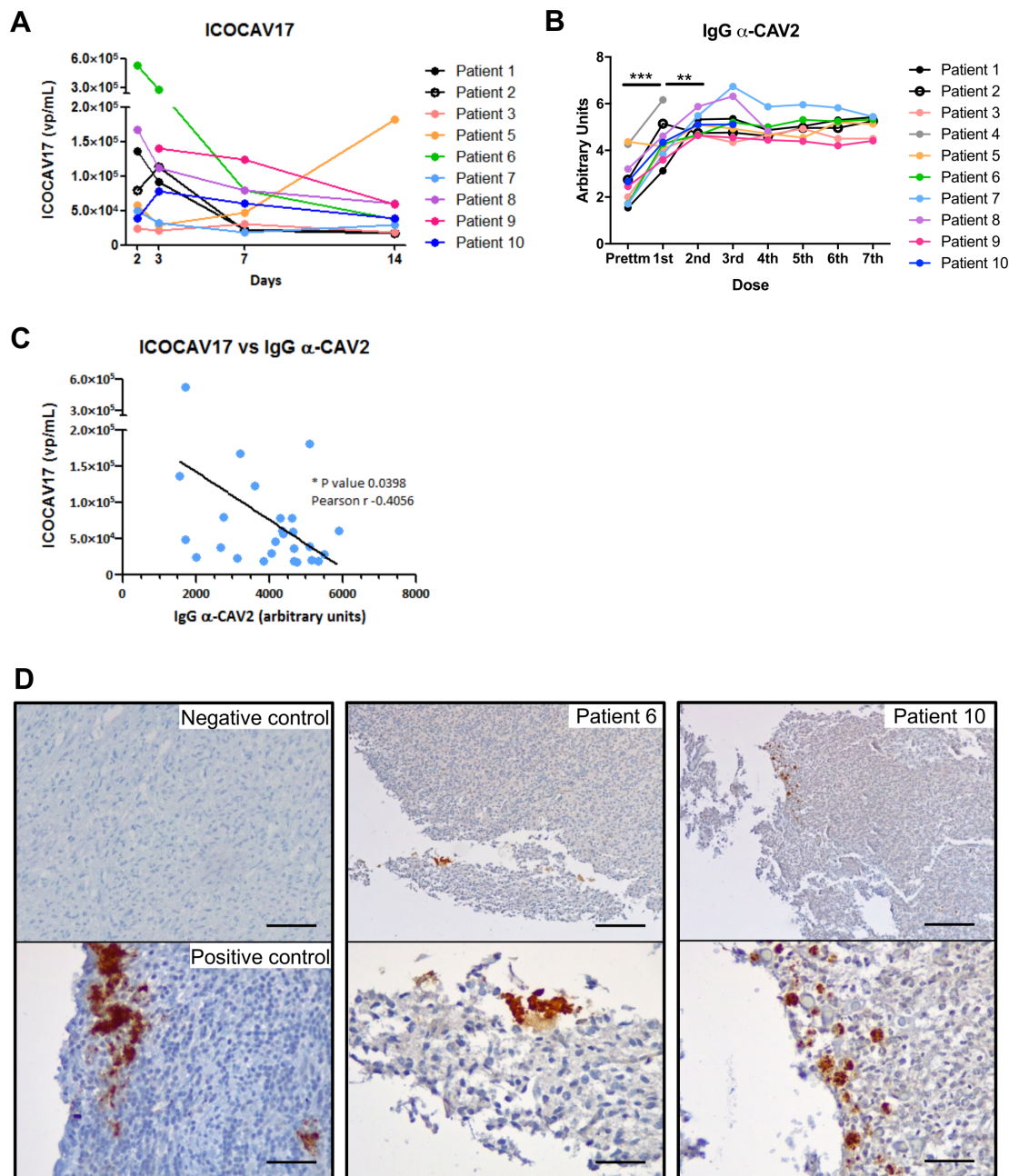


Figure 3 Oncolytic virus and antibody response. (A) Adenovirus detection during follow-up. Adenovirus presence analyzed by quantitative PCR (qPCR) in peripheral blood is shown. Quantification time refers to the time after the first day of treatment (day 0). Individual values from each patient are shown. (B) Specific antibodies. IgG α -CAV2 quantified by solid phase ELISA in the serum of canine patients during dCelyvir treatments. A Wilcoxon test was performed ($***p < 0.0001$; $**p < 0.005$). (C) Correlation between oncolytic adenovirus and specific antibodies was calculated by Pearson's correlation coefficient (r), using data from all available dogs up to the second week of treatment (14th day after treatment). Individual values (blue dots) and a regression line are shown. $*p < 0.05$. (D) The presence of adenovirus inside gliomas analyzed by immunohistochemistry. Representative images showing adenovirus-positive cells (brown) on formalin-fixed, paraffin-embedded-positive control tissue, and tumor necropsies from patients 6 and 10. Scale bars: 50 μ m (negative and positive controls), 200 μ m (top patients) and 50 μ m (bottom patients).

the second dose they tended to stabilize over the following treatments (figure 3B). Although the dogs had similar antibody trend, they showed greater differences in viral particles detected in blood (figure 3A–B). There was a negative correlation ($r = -0.4056$) between the ICOCAV17 particles in peripheral blood and the specific antibodies against CAV2 (figure 3C).

Immune response in peripheral blood

Cytokines in peripheral blood were quantified during the first 4 weeks by analysis with a multiplex cytokine panel to analyze whether the dCelyvir treatment could be modifying the dogs' cytokine secretion. No alterations in IL-2, IL-6, IL-7, IL-15, IL-18, GM-CSF, CCL2, or CXCL10 during the treatment were detected (figure 4). However, patient

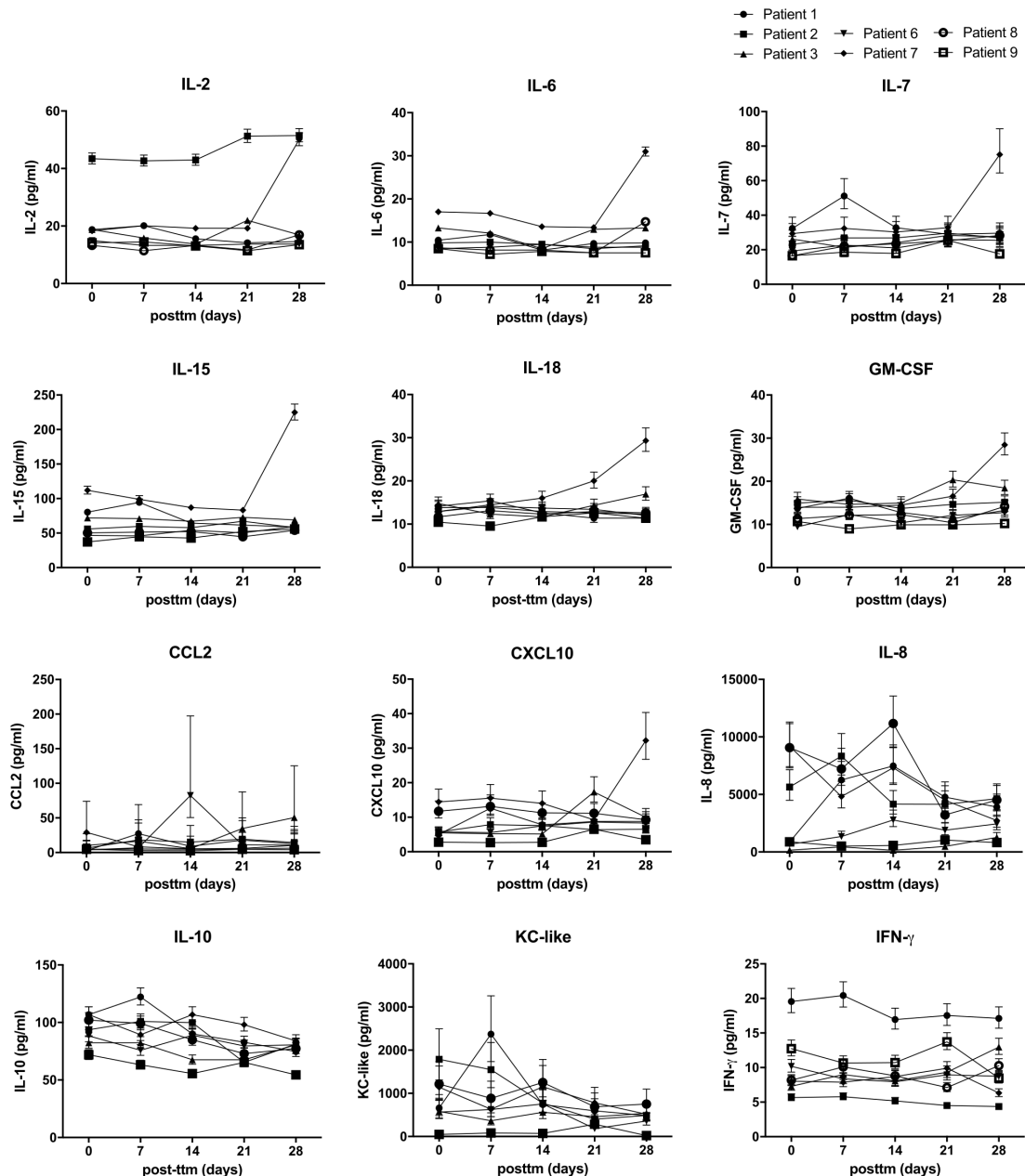


Figure 4 Cytokines in peripheral blood from treated patients quantified by a multiplex assay. Sera from treated dogs were analyzed prior to treatment (d0) and Weekly after the first four treatments (days 7, 14, 21, and 28) for IL-2, IL-6, IL-7, IL-15, IL-18, GM-CSF, CCL2, CXCL10, IL-8, IL-10, KC-like, and IFN- γ . Individual values are shown. GM-CSF, granulocyte-macrophage colony-stimulating factor.

7 showed an increase in IL-2, IL6, IL-7, IL-15, IL-18, GM-CSF, and CXCL10 levels after 4 weekly doses. Patient 2 had the highest IL-2 quantification before starting and during the entire treatment. Immune cell populations in peripheral blood were quantified by flow cytometry to assess whether the dCelyvir treatment was affecting the normal function of the immune system, but no significant differences in neutrophil, T cell, macrophage, or natural killer cell counts were observed (data not shown).

Tumor-infiltrating immune cells

Immunohistochemistry was performed to investigate whether the dCelyvir treatment could induce changes in

tumor-infiltrating lymphocytes (TILs), which could not be detected in two grade III oligodendrogliomas (table 2). In the rest of the dogs, lymphocytic infiltrates were found around glomeruloid vessels forming perivascular cuffs or as scattered cells within the tumor (online supplemental figure S4). The most prominent lymphocytic population was CD3⁺ TILs, in all tumors (mean of 36.05 cells/mm²) and increased considerably in GBM (118.2 cells/mm²) compared with grade III oligodendrogliomas (8.64 cells/mm²) (figure 5A and table 2). FOXP3⁺ lymphocytes were detected in 25% (2/8) of the evaluated samples and were particularly severe in the GBM. A low number of CD20⁺

**Table 2** Inflammatory pattern and quantification of TILs

Patient	Inflammatory pattern	TILs (mean)		
		FOXP3+	CD3+	CD20+
1	None	0	0	0
2	None	0	0	0
3	Perivascular+intratumoral	0	28	2.4
5	Perivascular+intratumoral	0	4.8	1.6
6	Perivascular+intratumoral	17.6	226	27.2
7	Perivascular+intratumoral	0	10.4	1.6
8	Perivascular	0	12.8	0.8
10	Intratumoral	1.6	6.4	3.2

TILs, tumor-infiltrating lymphocytes.

cells was observed (mean of 4.6 cells/mm²). Patient 6 showed the highest number of CD20+ cells, as occurred with other evaluated lymphocytic populations (figure 5A and table 2).

To determine whether the intratumor immune micro-environment could be affected by the dCelyvir treatment, a CIBERSORT algorithm that estimated TIL composition from bulk RNA expression data was employed (figure 5B). The dogs with SD (2/5) and PR (1/5) presented a tendency for reduced memory B-cell infiltration and increased B-cell activation. Similarly, a tendency to increased monocyte/macrophage lineage infiltration was observed in the dogs with SD and PR (figure 5C). Interestingly, dogs with osteolytic lesions (3/4) also presented changes in TIL composition, with a significant reduction in memory B cells and a higher infiltration of the monocyte/macrophage lineage (figure 5D).

DISCUSSION

In this study, 9/10 dogs were brachycephalic according to other reports that describe the predisposition of brachycephalic dog breeds to gliomas.^{20 24 26} The median time from the onset of clinical symptoms to diagnosis (40 days) agreed with previously reported values, as did the imaging characteristics.^{27 35} Therefore, our study population should be considered as a representative sample of spontaneous high-grade glioma in dogs.

The dCelyvir treatment was well tolerated, as we had previously reported with extracranial solid tumors.⁶ Only minor adverse effects (limb swelling and fatigue) were sporadically observed and were self-limiting or required short-term anti-inflammatory treatment. There were no significant changes in the complete blood count, and biochemical parameters were stable within the referenced ranges. The finding of adenovirus inside the tumors is evidence that dMSCs are effective in delivering of ICOCV17 into gliomas; but due to the strong hepatotropism of Ads, ICOCV17 could have accumulated in the liver, as previously reported with dCelyvir treatment.^{6 36} Despite the prevalence of microscopic lesions, especially previously reported chronic inflammatory responses in

different organs, the use of dCelyvir did not demonstrate significant pathological changes or clinical signs in the livers of dogs presenting extracranial solid tumors.^{6 36} Considering these findings with the biochemical abnormalities that patient 4 presented before the dCelyvir treatment, an undetected pre-existing liver disease (toxic hepatopathy secondary to phenobarbital and/or steroids, infectious hepatitis, or diffuse neoplasia) could be the cause of its clinical deterioration.

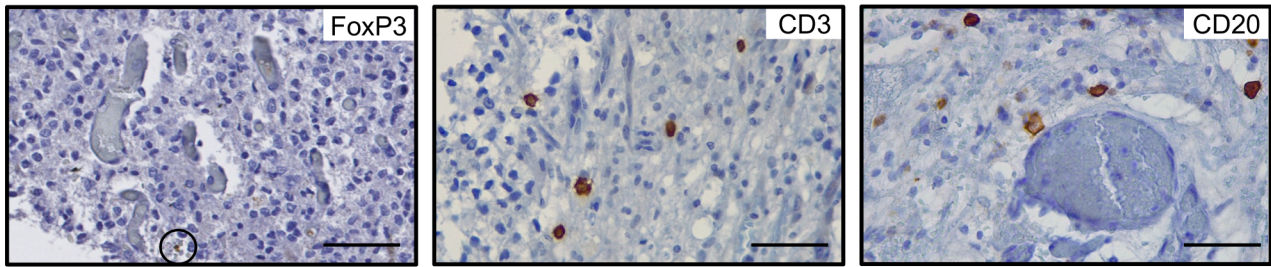
Radiation therapy has become the gold standard for treating canine high-grade glioma, with MSTs from 255 to 282 days; however, it is expensive and there are few hospitals that offer this therapy.²⁶ In dogs, lomustine has shown a benefit in MST from diagnosis when compared with palliative care (138 vs 35 days).³⁷ Interestingly, dCelyvir treatment shows a slight increase in MST from treatment (90 days) when compared with palliatively treated dogs (35 days)³⁷ or surgically treated dogs.³⁸ We have not found an association between MST and tumor volume or its localization; however, it is important to note that most of the patients presented large-sized tumors (>2 cm³).

Tumor size was increased after 2 months of treatment in 3 dogs (3/7) in which revision MRI was performed, which could be due to tumor cell proliferation and/or tumor pseudoprogression, the latter of which has been observed in humans with recurrent high-grade gliomas treated intratumorally with DNX-2401, a CRAd homologous to ICOCV17,¹² and in dogs with brain tumors treated with intrathecal Zika virus.³⁹ This phenomenon appeared soon after the start of treatment, followed by a progressive reduction in tumor size; however, the dogs' short survival time did not allow us to confirm that possibility in this study. Unfortunately, given that there are no consensus criteria for the analysis of immunotherapies in veterinary medicine, RAVNO criteria have been used even though they do not consider pseudoprogessions as do the immune-specific response criteria in human clinical practice, the Immune-related Response Evaluation Criteria in Solid Tumors and the Immune-related response criteria.

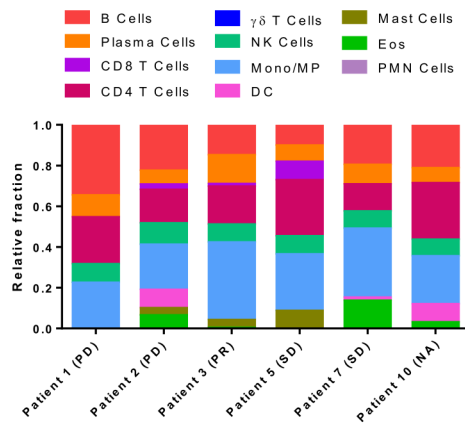
Severe skull bone resorption (calvarial erosion) was detected in 3 dogs (3/4) examined with CT soon before or after death. This event has been previously reported in dogs, although is an uncommon finding in humans with brain tumors.^{40 41} The proposed mechanisms are direct invasion of tumor cells into the skull, tumor pressure on the inner table of the skull, and the destruction caused by proteolytic enzymes secreted by the tumor cells.⁴¹ Calvarial erosion was found to be near the neoplasia but also distally and bilaterally (patients 3 and 7). There is the clinical impression that skull bone resorption in dogs with long-standing gliomas is much more frequent than that reported to date in the veterinary literature.

EIA-mutant human Ads demonstrated potent cytolytic effects in human gliomas^{42 43} and canine Ads in extracranial solid tumors, either administered intratumorally^{13 18} or carried by dMSCs, with higher clinical benefit.⁶ Although dCelyvir has been reported to reach an extracranial solid

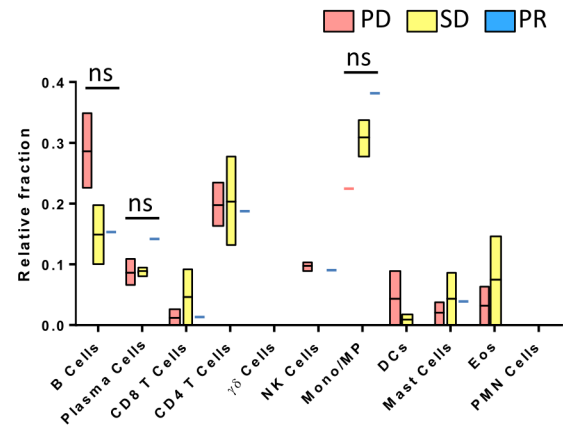
A



B



C



D

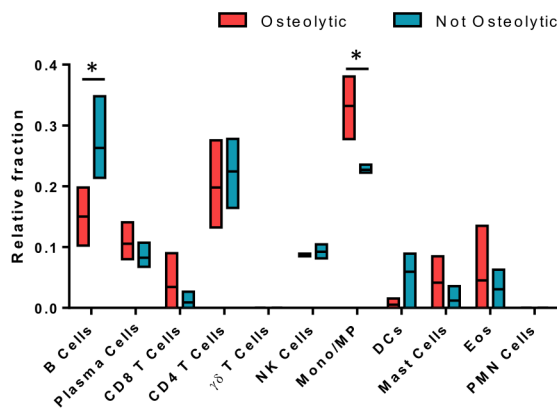


Figure 5 Intratumor immune microenvironment characterization after dCelyvir treatment. (A) The presence of immune cells inside gliomas analyzed by immunohistochemistry. Representative images showing immune cells (brown) on formalin-fixed, paraffin-embedded tumors at necropsies. Scale bars: 50 μ m. (B) Relative fraction of 11 types of TILs in 6 dogs estimated with CIBERSORT. (C) Immune cell relative fraction from patients depending on their clinical benefit, after dCelyvir treatment. (D) Immune cell relative fraction from patients, comparing those that present an osteolytic pattern at CT imaging (osteolytic) and those that do not (not osteolytic). Statistic test: Two-way ANOVA and Bonferroni's multiple comparison test; Alpha: 0.05; ns: not significant; * $p < 0.05$. ANOVA, analysis of variance; DC, dendritic cells; Eos, Eosinophils; Mono/MP, Monocyte/Macrophages; PD, progressive disease; PMN, polymorphonuclear cells; PR, partial response; SD, stable disease; TILs, tumor-infiltrating lymphocytes.

tumor in a canine patient,⁴⁴ this is the first time that systemically administered viral treatment has been shown to effectively reach the brain tumor and show biological activity, a fact of vital importance for the efficacy of the therapy. Despite that, the limited efficacy of dCelyvir in treating high-grade gliomas could have been due to (1) the specific characteristics of the immune system in the CNS; (2) the fact that the viral load reaching the tumor was reduced by the blood-brain barrier; (3) due to the MSC sequestration in the lungs

(or other organs); or (4) by the large tumor size at the time of inclusion in the study.^{45 46}

All dogs presented an increase in IgG α -CAV-2 until reaching a plateau after the second dCelyvir dose, in agreement with previous studies.^{6 13} The increase of the antibody levels did not preclude a clinical benefit in this study; there was a correlation between antiviral antibodies and ICOCV17 particles, suggesting that a lower concentration of antibodies could reduce the number of neutralized viral

particles, thereby allowing a higher oncolytic viral load. The use of an OV, against which the dogs have not been previously vaccinated, should be considered in the future to favor dCelyvir effectiveness.

The absent systemic inflammatory response observed in the cytokine profile in most of the dogs could indicate that ICOCV17 did not elicit an exaggerated systemic response, in contrast to other intrathecally injected viruses that increased IL-8, keratinocyte chemoattractant (KC)-like, and CCL2 in the serum of dogs with malignant intracranial tumors.³⁹ However, the intratumoral immune cells analysis of our treatment suggested that changes in TILs could be relevant in treatment response. The glioma composition of TILs in our treated dogs was according to that reported in non-treated dogs with gliomas, consisting in higher population of CD3+ and FoxP3+, compared with CD20+ TILs. Also, the number of TILs were increased in GBM compared with lower grade gliomas.¹⁹ However, dogs showing a clinical benefit such as SD or PR present a tendency for reduced memory B-cell infiltration and increased activated B cells and monocyte/macrophage-lineage cells infiltrated. It has now been proven that the tumor-infiltrating T lymphocytes play a critical role in controlling or promoting tumor growth, but the function of B lymphocytes is less clear, although recent data have indicated a critical role for tumor-infiltrating B-cells in immunotherapies.⁴⁷ Changes in TIL populations have also been observed in dogs with osteolytic lesions. However, osteoclasts can have a monocytic-macrophagic derivation,^{48–50} and dogs presenting an osteolytic pattern showed an increased relative fraction of this lineage. Thus, further studies should be performed to clarify these relationships.

In this study, dMSCs infected with a canine OV to treat high-grade gliomas in dogs were used without significant toxicities or adverse reactions. The increased MST compared with previous reports describing the prognosis of palliative treatment or surgery makes dCelyvir a candidate for combination therapy with surgery or different administration routes. These findings could be relevant for clinical trials being developed in humans, which are similar to this study, such as the phase Ib clinical trial using this cellular virotherapy in children, adolescents, and young adults with diffuse intrinsic pontine glioma (EudraCT 2020-004838-37) and the trial with the oncolytic adenovirus DNX-2401 in patients with recurrent high-grade glioma (NCT03896568). The reported data using dogs as a preclinical model could serve as a transition in the therapeutic development of human medicine and can potentially improve the success of subsequent clinical trials.

Author affiliations

¹Servicio de Neurología, Hospital Clínico Veterinario, Universidad Alfonso X el Sabio, Villanueva de la Cañada, Spain

²Servicio de Neurología, Hospital Veterinario VETSIA, Leganés, Spain

³Unidad de Biotecnología Celular, Instituto de Salud Carlos III, Madrid, Spain

⁴Molecular Genetics of Angiogenesis Group, Spanish National Centre for Cardiovascular Research (CNIC), Madrid, Spain

⁵Unitat de Patologia Murina i Comparada (UPMiC), Departament de Medicina

i Cirurgia Animals, Facultat de Veterinària, Networking Research Center on Bioengineering, Biomaterials and Nanomedicine (CIBER-BBN), Universitat Autònoma de Barcelona, Barcelona, Spain

⁶IDIBELL, Institut Català d'Oncologia, Barcelona, Spain

⁷Unidad de Investigación Biomédica (UIB-UAX), Universidad Alfonso X el Sabio, Villanueva de la Cañada, Spain

Twitter Stefano Gambera @GamberaStefano and Javier García-Castro @JavierGC280

Acknowledgements The authors would like to thank Miguel Ángel Rodríguez-Milla, Isabel Cubillo and Álvaro Morales from Unidad de Biotecnología Celular, Instituto de Salud Carlos III for their technical support in the study. The authors would also like to thank Dolores Pi, Ester Blasco and Tamara Rivero from Unitat de Patologia Murina i Comparada (UPMiC) at Universitat Autònoma de Barcelona, and for their technical support with the diagnosis and immunohistochemistry. The authors would also like to thank Pablo Delgado-Bonet from Universidad Alfonso X el Sabio for his help with the IHC images. The graphical abstract and figure 1 have been designed using images from Freepik.com, which have free license.

Contributors Conception and design: JG-C and AJP-B; Development of tools and methodology: AC, IM, RA, and AJP-B; Acquisition of data (provided animals, managed patients, diagnosis and provided facilities): AC, IM, MP, JG-C; Analysis and interpretation of data (imaging, statistical analysis and computational analysis): IM, SG, MP, JG-C and AJP-B; Writing the paper: AC, IM, SG and AJP-B; Review the paper: AC, IM, SG, MP, RA, JG-C and AJP-B. Guarantor: JG-C

Funding This work was funded by Instituto de Salud Carlos III (PI14CIII/00005 and PI17CIII/00013 grants to JG-C), Consejería de Educación, Juventud y Deporte of Comunidad de Madrid (P2017/BMD-3692 grant to JG-C), the Madrid Regional Government (CellCAM; P2010/BMD-2420 to JG-C), the Asociación Pablo Ugarte, and the Asociación AFANION. This work was also supported by Universidad Alfonso X el Sabio and Santander Universidades-Fundación Universidad Alfonso X el Sabio (1010909 grant to AJP-B).

Competing interests None declared.

Patient consent for publication Not applicable.

Provenance and peer review Not commissioned; externally peer reviewed.

Data availability statement All data relevant to the study are included in the article or uploaded online as supplemental information. Not applicable.

Supplemental material This content has been supplied by the author(s). It has not been vetted by BMJ Publishing Group Limited (BMJ) and may not have been peer-reviewed. Any opinions or recommendations discussed are solely those of the author(s) and are not endorsed by BMJ. BMJ disclaims all liability and responsibility arising from any reliance placed on the content. Where the content includes any translated material, BMJ does not warrant the accuracy and reliability of the translations (including but not limited to local regulations, clinical guidelines, terminology, drug names and drug dosages), and is not responsible for any error and/or omissions arising from translation and adaptation or otherwise.

Open access This is an open access article distributed in accordance with the Creative Commons Attribution Non Commercial (CC BY-NC 4.0) license, which permits others to distribute, remix, adapt, build upon this work non-commercially, and license their derivative works on different terms, provided the original work is properly cited, appropriate credit is given, any changes made indicated, and the use is non-commercial. See <http://creativecommons.org/licenses/by-nc/4.0/>.

ORCID iDs

Ana Cloquell <http://orcid.org/0000-0002-1400-6134>

Isidro Mateo <http://orcid.org/0000-0002-2667-9459>

Stefano Gambera <http://orcid.org/0000-0003-2998-8502>

Javier García-Castro <http://orcid.org/0000-0001-7604-1640>

Ana Judith Perisé-Barrios <http://orcid.org/0000-0002-0136-3968>

REFERENCES

- 1 Sánchez D, Cesarman-Maus G, Amador-Molina A, *et al.* Oncolytic viruses for canine cancer treatment. *Cancers* 2018;10:404.
- 2 Russell L, Peng KW, Russell SJ, *et al.* Oncolytic viruses: priming time for cancer immunotherapy. *BioDrugs* 2019;33:485–501.
- 3 Tähtinen S, Grönberg-Vähä-Koskela S, Lumen D, *et al.* Adenovirus improves the efficacy of adoptive T-cell therapy by recruiting immune cells to and promoting their activity at the tumor. *Cancer Immunol Res* 2015;3:915–25.
- 4 Woller N, Gürlevik E, Fleischmann-Mundt B, *et al.* Viral infection of tumors overcomes resistance to PD-1-immunotherapy by

- broadening Neoantigenome-directed T-cell responses. *Mol Ther* 2015;23:1630–40.
- 5 Raja J, Ludwig JM, Gettinger SN, *et al.* Oncolytic virus immunotherapy: future prospects for oncology. *J Immunother Cancer* 2018;6:140.
 - 6 Cejalvo T, Perisé-Barrios AJ, Del Portillo I, *et al.* Remission of spontaneous canine tumors after systemic cellular Viroimmunotherapy. *Cancer Res* 2018;78:4891–901.
 - 7 Morales-Molina A, Rodríguez-Milla Miguel Ángel, Gimenez-Sanchez A, *et al.* Cellular Virotherapy Increases Tumor-Infiltrating Lymphocytes (TIL) and Decreases their PD-1⁺ Subsets in Mouse Immunocompetent Models. *Cancers* 2020;12:1920. doi:10.3390/cancers12071920
 - 8 Guedan S, Rojas JJ, Gros A, *et al.* Hyaluronidase expression by an oncolytic adenovirus enhances its intratumoral spread and suppresses tumor growth. *Mol Ther* 2010;18:1275–83.
 - 9 Ulasov IV, Borovjagin AV, Schroeder BA, *et al.* Oncolytic adenoviruses: a thorny path to glioma cure. *Genes Dis* 2014;1:214–26.
 - 10 Kiyokawa J, Wakimoto H. Preclinical and clinical development of oncolytic adenovirus for the treatment of malignant glioma. *Oncolytic Virother* 2019;8:27–37.
 - 11 Bush NAO, Chang SM, Berger MS. Current and future strategies for treatment of glioma. *Neurosurg Rev* 2017;40:1–14.
 - 12 Lang FF, Conrad C, Gomez-Manzano C, *et al.* Phase I study of DNX-2401 (Delta-24-RGD) oncolytic adenovirus: replication and immunotherapeutic effects in recurrent malignant glioma. *J Clin Oncol* 2018;36:1419–27.
 - 13 Martín-Carrasco C, Delgado-Bonet P, Tomeo-Martín BD, *et al.* Safety and efficacy of an oncolytic adenovirus as an immunotherapy for canine cancer patients. *Vet Sci* 2022;9:327. doi:10.3390/vetsci9070327
 - 14 Gállego Pérez-Larraya J, Garcia-Moure M, Labiano S, *et al.* Oncolytic DNX-2401 virus for pediatric diffuse intrinsic pontine glioma. *N Engl J Med* 2022;386:2471–81.
 - 15 Ferguson MS, Lemoine NR, Wang Y. Systemic delivery of oncolytic viruses: hopes and hurdles. *Adv Virol* 2012;2012:1–14.
 - 16 García-Castro J, Alemany R, Cascalló M, *et al.* Treatment of metastatic neuroblastoma with systemic oncolytic virotherapy delivered by autologous mesenchymal stem cells: an exploratory study. *Cancer Gene Ther* 2010;17:476–83.
 - 17 Ruano D, López-Martín JA, Moreno L, *et al.* First-In-Human, First-in-Child trial of autologous MscS carrying the oncolytic virus Icovir-5 in patients with advanced tumors. *Mol Ther* 2020;28:1033–42.
 - 18 Laborda E, Puig-Saus C, Rodríguez-García A, *et al.* A pRb-responsive, RGD-modified, and hyaluronidase-armed canine oncolytic adenovirus for application in veterinary oncology. *Mol Ther* 2014;22:986–98.
 - 19 Amin SB, Anderson KJ, Boudreau CE, *et al.* Comparative molecular life history of spontaneous canine and human gliomas. *Cancer Cell* 2020;37:243–57.
 - 20 José-López R, Gutierrez-Quintana R, de la Fuente C, *et al.* Clinical features, diagnosis, and survival analysis of dogs with glioma. *J Vet Intern Med* 2021;35:1902–17.
 - 21 Delgado-Bonet P, Tomeo-Martín BD, Delgado-Bonet B, *et al.* Intracranial virotherapy for a canine hemangioma. *Int J Mol Sci* 2022;23:11677. doi:10.3390/ijms231911677
 - 22 Connolly NP, Shetty AC, Stokum JA, *et al.* Cross-species transcriptional analysis reveals conserved and host-specific neoplastic processes in mammalian glioma. *Sci Rep* 2018;8:1180.
 - 23 Boudreau CE, York D, Higgins RJ, *et al.* Molecular signalling pathways in canine gliomas. *Vet Comp Oncol* 2017;15:133–50.
 - 24 Song RB, Vite CH, Bradley CW, *et al.* Postmortem evaluation of 435 cases of intracranial neoplasia in dogs and relationship of neoplasm with breed, age, and body weight. *J Vet Intern Med* 2013;27:1143–52.
 - 25 LeBlanc AK, Mazcko CN. Improving human cancer therapy through the evaluation of pet dogs. *Nat Rev Cancer* 2020;20:727–42.
 - 26 Dickinson PJ. Advances in diagnostic and treatment modalities for intracranial tumors. *J Vet Intern Med* 2014;28:1165–85.
 - 27 Debreuque M, De Fornel P, David I, *et al.* Definitive-intent uniform megavoltage fractionated radiotherapy protocol for presumed canine intracranial gliomas: retrospective analysis of survival and prognostic factors in 38 cases (2013–2019). *BMC Vet Res* 2020;16:412.
 - 28 Koehler JW, Miller AD, Miller CR, *et al.* A revised diagnostic classification of canine glioma: towards validation of the canine glioma patient as a naturally occurring preclinical model for human glioma. *J Neuropathol Exp Neurol* 2018;77:1039–54.
 - 29 MacNeill AL. On the potential of oncolytic virotherapy for the treatment of canine cancers. *Oncolytic Virother* 2015;4:95–107.
 - 30 Alonso-Miguel D, Valdivia G, Guerrero D, *et al.* Neoadjuvant in situ vaccination with cowpea mosaic virus as a novel therapy against canine inflammatory mammary cancer. *J Immunother Cancer* 2022;10.
 - 31 Rossmeisl JH, Garcia PA, Daniel GB, *et al.* Invited review--neuroimaging response assessment criteria for brain tumors in veterinary patients. *Vet Radiol Ultrasound* 2014;55:115.
 - 32 Louis DN, Ohgaki H, Wiestler OD, *et al.* The 2007 WHO classification of tumours of the central nervous system. *Acta Neuropathol* 2007;114:97–109.
 - 33 Higgins RJ, Bollen AW, Dickinson PJ. Tumors of the nervous system. *Tumors in Domestic Animals* 2016:834–91.
 - 34 Chen B, Khodadoust MS, Liu CL, *et al.* Profiling tumor infiltrating immune cells with CIBERSORT. *Methods Mol Biol* 2018;1711:243–59.
 - 35 Kishimoto TE, Uchida K, Chambers JK, *et al.* A retrospective survey on canine intracranial tumors between 2007 and 2017. *J Vet Med Sci* 2020;82:77–83.
 - 36 Gómez A, Sardón D, Cejalvo T, *et al.* Biodistribution analysis of oncolytic adenoviruses in canine patient necropsy samples treated with cellular virotherapy. *Mol Ther Oncolytics* 2020;18:525–34.
 - 37 Moirano SJ, Dewey CW, Wright KZ, *et al.* Survival times in dogs with presumptive intracranial gliomas treated with oral lomustine: a comparative retrospective study (2008–2017). *Vet Comp Oncol* 2018;16:459–66.
 - 38 Suñol A, Mascort J, Font C, *et al.* Long-term follow-up of surgical resection alone for primary intracranial rostral tentorial tumors in dogs: 29 cases (2002–2013). *Open Vet J* 2017;7:375–83.
 - 39 Kaid C, Madi RADS, Astray R, *et al.* Safety, tumor reduction, and clinical impact of Zika virus injection in dogs with advanced-stage brain tumors. *Mol Ther* 2020;28:1276–86.
 - 40 Cunningham DA, Lowe LH, Shao L, *et al.* Neuroradiologic characteristics of astroblastoma and systematic review of the literature: 2 new cases and 125 cases reported in 59 publications. *Pediatr Radiol* 2016;46:1301–8.
 - 41 Recio A, de la Fuente C, Pumarola M, *et al.* Magnetic resonance imaging and computed tomographic characteristics of a glioma causing calvarial erosion in a dog. *Vet Radiol Ultrasound* 2019;60:E1–5.
 - 42 Fueyo J, Gomez-Manzano C, Alemany R, *et al.* A mutant oncolytic adenovirus targeting the Rb pathway produces anti-glioma effect in vivo. *Oncogene* 2000;19:2–12.
 - 43 Alonso MM, Cascallo M, Gomez-Manzano C, *et al.* ICOVIR-5 shows E2F1 addiction and potent antiglioma effect in vivo. *Cancer Res* 2007;67:8255–63.
 - 44 Delgado-Bonet P, Tomeo-Martín BD, Ortiz-Díez G, *et al.* Tumor-homing of mesenchymal stem cells infected with oncolytic virus in a canine patient. *Vet Sci* 2022;9:285.
 - 45 Abdi Z, Eskandary H, Nematollahi-Mahani SN. Effects of two types of human cells on outgrowth of human glioma in rats. *Turk Neurosurg* 2018;28:19–28.
 - 46 Conaty P, Sherman LS, Naaldijk Y, *et al.* Methods of mesenchymal stem cell homing to the blood-brain barrier. *Methods Mol Biol* 2018;1842:81–91.
 - 47 Downs-Canner SM, Meier J, Vincent BG, *et al.* B cell function in the tumor microenvironment. *Annu Rev Immunol* 2022;40:169–93.
 - 48 Madel M-B, Ibáñez L, Wakkach A, *et al.* Immune function and diversity of osteoclasts in normal and pathological conditions. *Front Immunol* 2019;10:1408.
 - 49 Keller A, Zarb Y. Reply: osteoclast imbalance in primary familial brain calcification: evidence for its role in brain calcification. *Brain* 2020;143:e2.
 - 50 Zarb Y, Weber-Stadlbauer U, Kirschenbaum D, *et al.* Ossified blood vessels in primary familial brain calcification elicit a neurotoxic astrocyte response. *Brain* 2019;142:885–902.

Figure S1

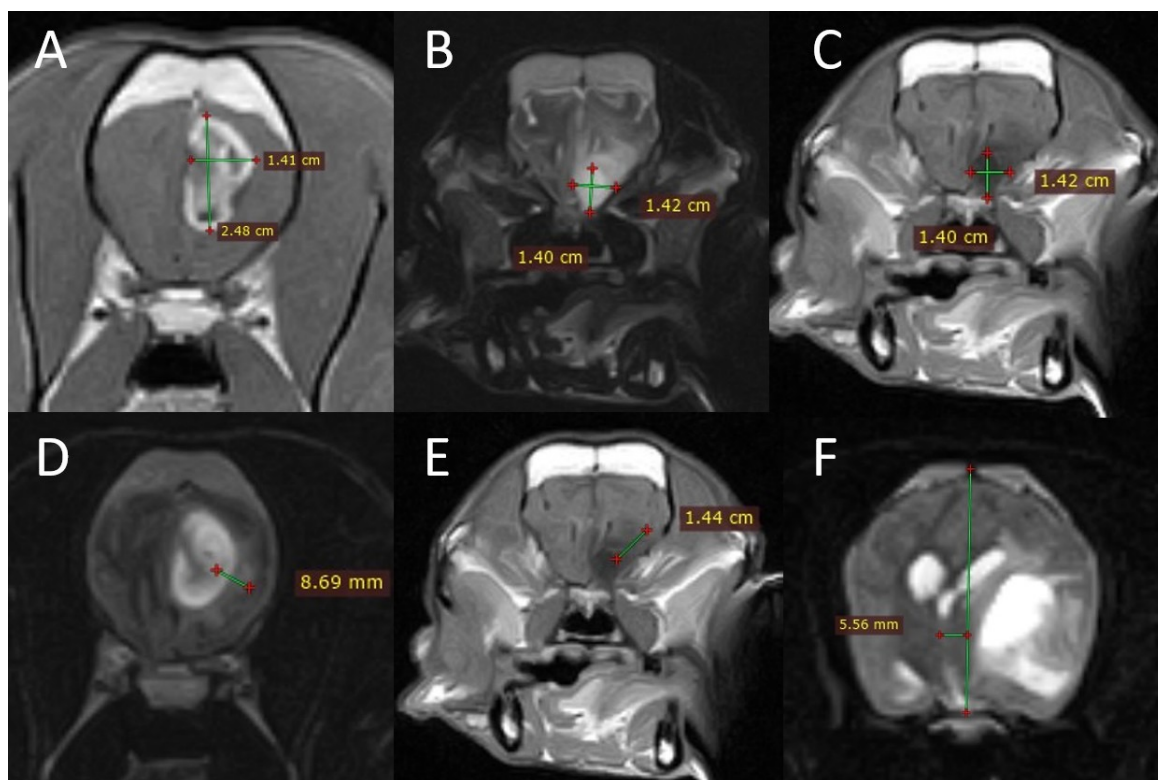
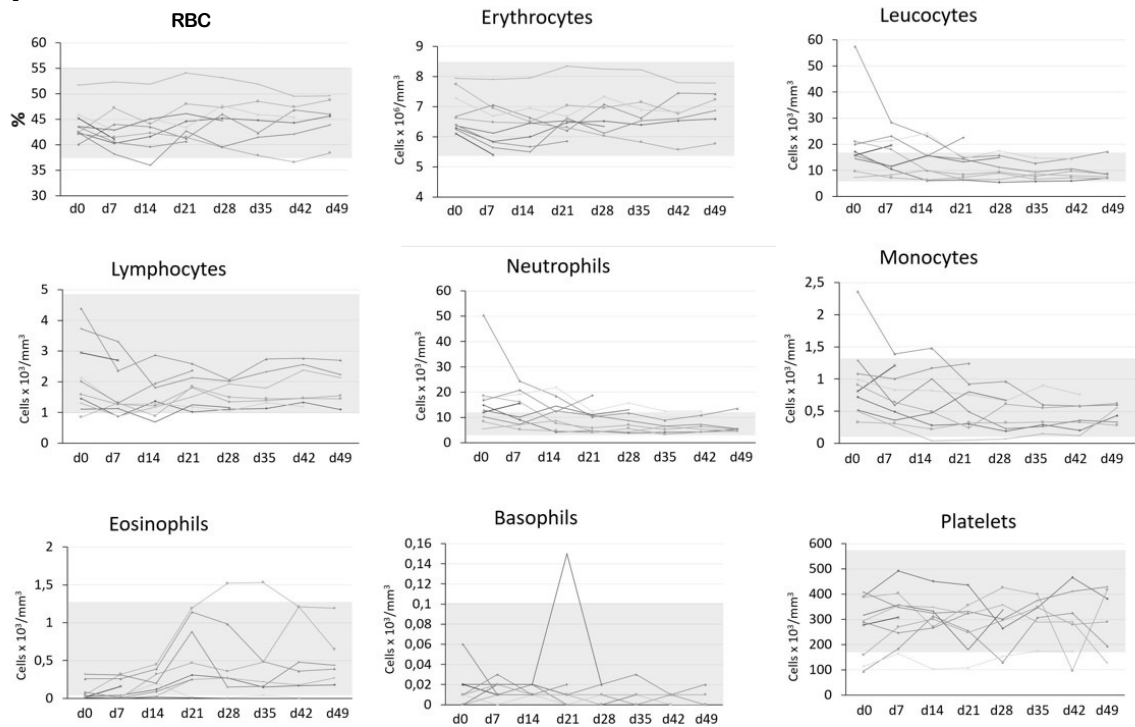


Figure S2

A



B

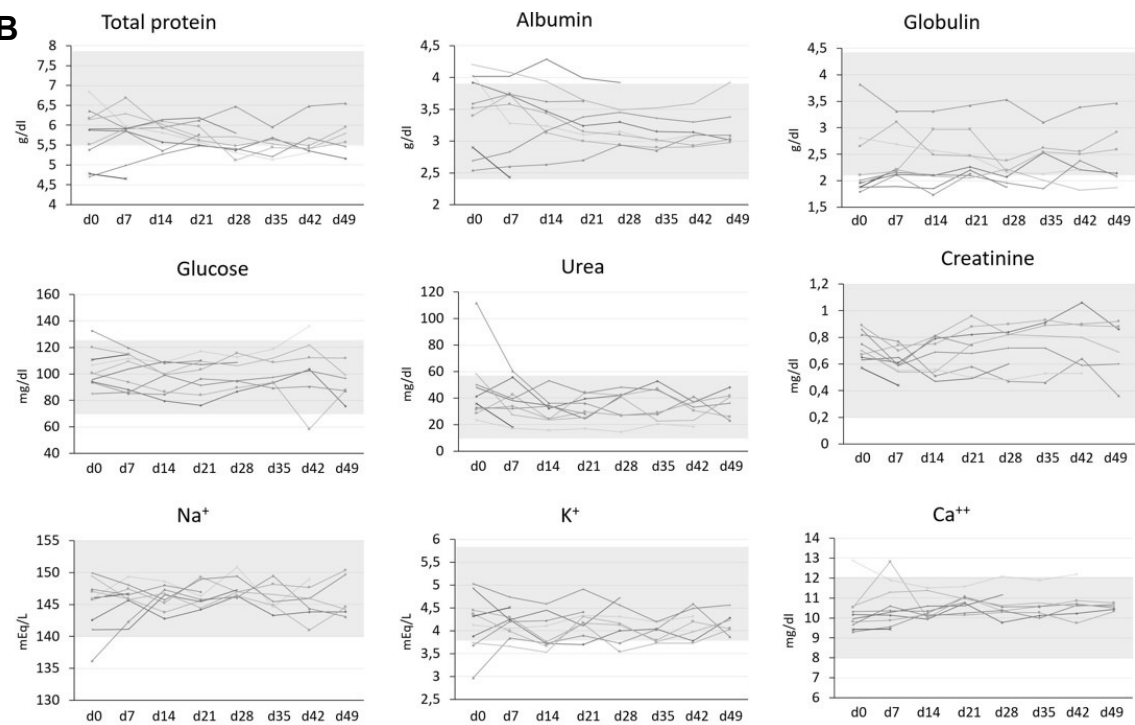


Figure S2

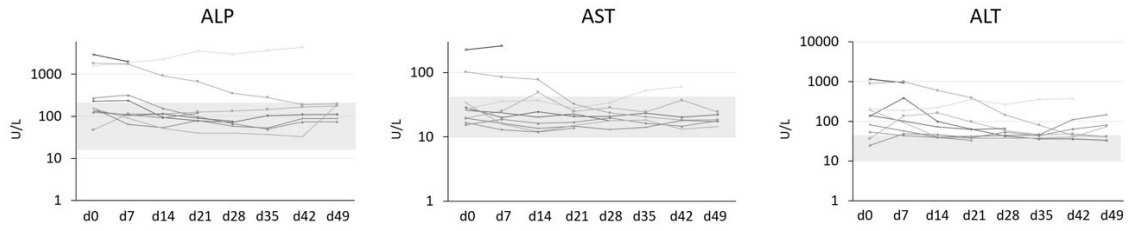
C

Figure S3

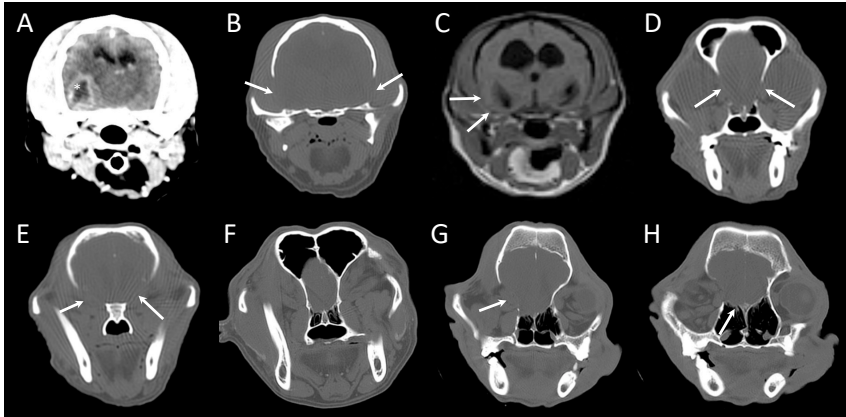
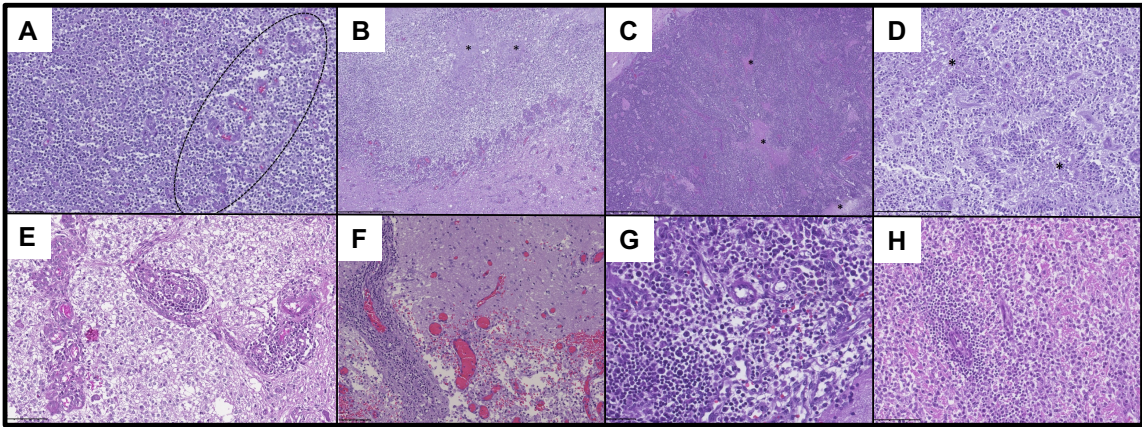


Figure S4



Supplemental material and methods

Magnetic resonance imaging

The standardized protocol included sagittal and transverse T2W images, dorsal fluid-attenuated inversion recovery (FLAIR) sequences and transverse, sagittal and dorsal T1W pre- and post-contrast images. Each tumor was categorized according to their location, shape (round, ovoid or multilobular), and signal intensity relative to grey matter in each sequence, signal homogeneity, grow pattern (compressive or infiltrative) and margins (well delineated or diffuse). On post-contrast T1W images (T1W+Gd), enhancement was categorized as absent, weak, or intense. Uniformity of contrast enhancement was characterized as homogeneous, heterogeneous, or ring-like enhancement. The largest area of the tumor was calculated as the product of the longest perpendicular diameters across a contrast-enhancing lesion in a transverse plane. In cases with limited or no enhancement, reasonable estimates of the extent considered spatial changes in relation to normal anatomy and T1W and T2W parenchymal intensity patterns. Peritumoral edema was defined as parenchymal hyperintensity on FLAIR or T2W or hypointense T1W imaging sequences adjacent to the boundary of the mass. If present, it was categorized as mild if it extended ≤ 10 mm or severe if it extended > 10 mm beyond the tumor margin. Other variables attributed to the tumor's mass effect were also recorded, including the presence or absence of ventricular collapse or dilation, transtentorial or foramen magnum cerebral herniation and midline shift. The degree of midline shift was also calculated by visual identification of the point of maximal deviation in a T2W transverse image that allowed the creation of a

digital line through the vertical axis beginning at the dorsal sagittal sinus, extending along the midline, and ending at the base of the cranium. A second perpendicular line was created from the vertical line to the point of maximal deviation of the midline and measured as an absolute number.

Histopathology, diagnosis, and immunohistochemistry

Fixed tissues from 8 necropsies were paraffin embedded after 10% neutral formalin fixation during at least 24 h. Morphological evaluation was performed on 5µm paraffin-embedded sections stained with hematoxylin and eosin. The presence of necrosis, extracellular matrix degradation, vascular proliferation, mucinous secretion, and hemorrhages were graded as mild, moderate, or severe, compared with 10 untreated gliomas from the tissue bank of the Murine and Comparative Pathology Unit (*Unitat de Patologia Murina i Comparada*, UPMiC) at the Autonomous University of Barcelona (*Universitat Autònoma de Barcelona*).

Samples were deparaffined and treated with 3% hydrogen peroxide for 35 min. Samples were incubated with 30% normal goat serum for 1 h at room temperature and overnight with primary antibodies at 4 °C: rabbit antiovine glial fibrillary acidic protein (GFAP, Dako Denmark Z0334) and rabbit polyclonal to recombinant mouse Olig2 (Olig2, Merck Millipore AB 9610). To characterize the tumor-infiltrating lymphocytes (TIL) population, antibodies for T lymphocytes CD3 (rabbit antihuman polyclonal, Dako A0452), B lymphocytes CD20 (rabbit antihuman polyclonal, thermo Fisher PA5-32313) and Treg lymphocytes FOXP3 (forkhead box P3) (mouse antihuman monoclonal, eBioscience 14-7979) were

used. To detect ICOCaV, a polyclonal anti-Ad5 was incubated overnight (Abcam ab6982). Samples were then incubated for 40 min at room temperature with a Envision-horseradish peroxidase (Dako REAL Envision-HRP) followed by incubation with 3'-diaminobenzidine for 10 min and counterstaining in hematoxylin for 3 s. Canine lymphoid tissue was used as a positive control for CD3, CD20, and FOXP3. For each slide, areas with the highest concentration of immunolabeled cells were identified and, within these, 5 round areas of 0.257 mm² were selected for quantification (magnification 40×). The CD3⁺, CD20⁺ and FOXP3⁺ lymphocyte counts were determined. Given that cellularity was low in all selected fields, a mean value was obtained for the lymphocyte counts of all areas assessed in each tumor, which was ultimately expressed as the number of positive cells per 0.257 mm² of tissue.

Supplemental Table

Table S1. Magnetic resonance imaging (MRI) summary and timing.

Patient	1 st MRI		2 nd MRI		Variation		S-Dx	Dx to dCelyvir	dCelyvir to death	S-D
	mm ²	Midline shift (mm)	mm ²	Midline shift (mm)	Tumor growth (%)	Midline shift (%)				
1	113	2.8	398	4.7	+251	+65	28	14	168	210
2	97	1.8	199	1.9	+105	+3	2	36	90	128
3	339	1.8	48	1.5	-86	-21	14	4	77	95
4	163	1.7	N/A	N/A	N/A	N/A	43	39	20	102
5	350	3.3	308	2.76	-12	-16	230	6	122	358
6	307	4	229	8.6	-25	+116	4	6	147	157
7	380	5.7	410	5.9	+8	+3	61	11	112	184
8	670	5.6	N/A	N/A	N/A	N/A	3	10	32	45
9	337	2.8	82	0	-76	-26	6	22	177	205
10	57	0	N/A	N/A	N/A	N/A	17	29	26	72

Changes are indicated as tumor growth (%) and variations in midline shift (%) from first to second MRI. S, symptoms; Dx, diagnosis; ttm, treatment; S-Dx, days from symptom onset to diagnosis; Dx-ttm, days from diagnosis to treatment; ttm-D, days from treatment to death; S-D, days from symptom onset to death; N/A, not available.